Rayleigh-Quotient and Iterative-Threshold-Test-Based Blind TOA Estimation for IR-UWB Systems

Bin Shen, Chengshi Zhao, Taiping Cui, and Kyungsup Kwak

This letter proposes a non-coherent blind time-of-arrival (TOA) estimation scheme for impulse radio ultra-wideband systems. The TOA estimation is performed in two consecutive phases: the Rayleigh-quotient theorem-based coarse-signal acquisition (CSA) and the iterative-threshold-test-based fine time estimation (FTE). The proposed scheme serves in a blind manner without demanding any a priori knowledge of the channel and the noise. Analysis and simulations demonstrate that the proposed scheme significantly increases the signal detection probability in CSA and ameliorates the TOA estimation accuracy in FTE.

Keywords: Rayleigh quotient, iterative-threshold test, TOA estimation, impulse radio ultra-wideband (IR-UWB).

I. Introduction

In recent years, energy-detection (ED)-based non-coherent time-of-arrival estimation (TOAE) schemes have been used for impulse radio ultra-wideband (IR-UWB) systems with simple circuitry [1], [2] (see references in [1] and [2]). Requiring no local template waveform generation and operating at the sub-Nyquist sampling rate, ED considerably facilitates practical system implementation and achieves cost-efficient devices. However, due to the extremely low duty cycle of IR-UWB signals, the performance of non-coherent TOAE is vulnerable to aggregate noise effects.

We propose a blind non-coherent TOAE scheme which is carried out in two consecutive steps: the Rayleigh-quotient (RQ)-based coarse signal acquisition (CSA) and the iterative-threshold-test (ITT)-based fine time estimation (FTE). We first derive the optimal combining weights to maximize the probability of coarsely capturing the IR-UWB signal in the CSA stage. Subsequently, an ITT is performed in the FTE phase to obtain the final TOAE with a refined time granularity.

Manuscript received Oct. 6, 2009; revised Nov. 18, 2009; accepted Nov. 26, 2009.
This work was supported by Inha University Research Grant, Rep. of Korea.
Bin Shen (phone: +82 32 864 8935, email: shenbinem@gmail.com), Chengshi Zhao (email: zhaochengshi@gmail.com), Taiping Cui (email: cuitaiping@gmail.com), and Kyungsup Kwak (email: kskwak@inha.ac.kr) are with the Graduate School of IT and Telecommunications, Inha University, Incheon, Rep. of Korea.
doi:10.4218/etrij.10.0209.0421

II. System Model

Let the received IR-UWB signal be represented as

$$y(t) = \sum_{i=-\infty}^{\infty} d_i^{(rp)} \varpi_{\text{mp}}(t - iT_{\text{f}} - c_i T_{\text{c}} - \tau_{\text{toa}}) + v(t), \quad (1)$$

where the frame index and duration are denoted by i and T_{f}, respectively; T_{c} is the chip duration; and τ_{toa} is the actual TOA of the received signal. The effective pulse response after the multipath channel is $\varpi_{\text{mp}}(t)$. With large enough pre-filter bandwidth W, $v(t)$ is the white Gaussian noise with zero mean and power spectral density N_0. Time-hopping codes $c_i \in \{0, 1, \cdots, N_{\text{h}} - 1\}$ are assigned to different users with $N_{\text{h}} = T_{\text{f}} / T_{\text{c}}$. Random-polarity codes $d_i^{(rp)} \in \{\pm 1\}$ are used to smooth the spectrum. Note that no modulation is considered and we only investigate the single-user scenario since we employ an ED-based TOAE scheme [2].

In CSA, each observation interval T_{f} is partitioned into N subframes with equal length T_{sf}. An integrate-and-dump square-law device serves to collect the received signal energy samples within each sampling duration T_{b},

$$y_{i,n} = \int_{t_{\text{s}}+(n-1)T_{\text{sf}}+iT_{\text{b}}}^{t_{\text{s}}+(n-1)T_{sf}+(i-1)T_{\text{b}}} |y(t)|^2 dt, \ 1 \le n \le N, 1 \le i \le M, \quad (2)$$

where t_{s} is the arbitrary starting time of the TOAE operation, the aggregate $M \times N$ matrix is $\mathbf{Y} = [\boldsymbol{y}_1, \boldsymbol{y}_2, \cdots, \boldsymbol{y}_N]$ with entry $[\mathbf{Y}]_{in} = y_{i,n}$. Hereafter, $T_{\text{sf}}=MT_{\text{b}}=KmT_{\text{b}}$, where each T_{sf} is further divided into K segments for weight-setting in the CSA.

III. Rayleigh-Quotient-Based CSA

The TOAE is first carried out in the CSA stage, on the order of $-T_{\text{sf}}+\tau_{\text{toa}}<\hat{\tau}_{\text{toa}}<\tau_{\text{toa}}+T_{\text{sf}}$. We incorporate an optimal weighting process into the CSA, in which the test statistics are

$$\boldsymbol{r}=\text{vecdiag}(\mathbf{Y}^T\breve{\boldsymbol{\omega}}), \tag{3}$$

where $\boldsymbol{r}=[r_1,r_2,\cdots,r_N]^T$ and $\breve{\boldsymbol{\omega}}=\boldsymbol{\omega}\otimes\mathbf{1}_m$. Hereby, $\mathbf{1}_m$ is a column vector of m ones, $\boldsymbol{\omega}=[\boldsymbol{\omega}_1,\boldsymbol{\omega}_2,\cdots,\boldsymbol{\omega}_N]$ is the target weight matrix with $\boldsymbol{\omega}_n=[\omega_{1,n},\omega_{2,n},\cdots,\omega_{K,n}]^T$, $\otimes$ is the Kronecker product, and vecdiag(•) creates a column vector from the main diagonals of its argument matrix.

The CSA is achieved as

$$j=\arg\max_{n\in\{1,2,\cdots,N\}}\boldsymbol{r}, \tag{4}$$

which indicates that the j-th subframe is determined to contain most of the IR-UWB signal energy among the N subframes.

According to the central limit theorem, when $2mT_{\text{b}}W$ is asymptotically large, r_n complies with Gaussian distributions as

$$E[r_n]=\begin{cases}\boldsymbol{\omega}_n^T\mathbf{u}_0, & \\ \boldsymbol{\omega}_n^T\mathbf{u}_{1,n}, & \end{cases}\quad Var[r_n]=\begin{cases}\boldsymbol{\omega}_n^T\boldsymbol{\Sigma}_0\boldsymbol{\omega}_n, & \mathcal{H}_{0,n},\\ \boldsymbol{\omega}_n^T\boldsymbol{\Sigma}_{1,n}\boldsymbol{\omega}_n, & \mathcal{H}_{1,n},\end{cases} \tag{5}$$

where $\boldsymbol{u}_0=mN_0T_{\text{b}}W\mathbf{1}_K$, $\boldsymbol{u}_{1,n}=\boldsymbol{u}_0+E[\boldsymbol{\theta}_n]$, and the IR-UWB signal energies are $\boldsymbol{\theta}_n=[\theta_{1,n},\theta_{2,n},\cdots,\theta_{K,n}]^T$, $\theta_{k,n}\ge 0$. $\boldsymbol{\Sigma}_0$ and $\boldsymbol{\Sigma}_{1,n}$ are the covariance matrices of r_n under null hypothesis $\mathcal{H}_{0,n}$ and alternative hypothesis $\mathcal{H}_{1,n}$, respectively.

Suppose the n-th subframe contains the IR-UWB signal component, the signal-to-noise ratio (SNR) of r_n is

$$\Gamma_n(\boldsymbol{\omega}_n)=\sqrt{\frac{mT_bW(E[r_n|\mathcal{H}_{1,n}]-E[r_n|\mathcal{H}_{0,n}])^2}{Var[r_n|\mathcal{H}_{0,n}]}}. \tag{6}$$

We realize that $\Gamma_n^2(\boldsymbol{\omega}_n)$ is actually a general Rayleigh quotient (GRQ) [3]:

$$\Gamma_n^2(\boldsymbol{\omega}_n)=\alpha\mathcal{R}(\boldsymbol{\omega}_n;\mathbf{R}_\theta,\boldsymbol{\Sigma}_0)\triangleq\alpha\frac{\boldsymbol{\omega}_n^T\mathbf{R}_\theta\boldsymbol{\omega}_n}{\boldsymbol{\omega}_n^T\boldsymbol{\Sigma}_0\boldsymbol{\omega}_n}, \tag{7}$$

where $\alpha=mT_{\text{b}}W$ and $\mathbf{R}_\theta=E[\boldsymbol{\theta}_n\boldsymbol{\theta}_n^T]$. The optimal weights $\boldsymbol{\omega}_{n,\text{opt}}$ are consequently the ones maximizing $\mathcal{R}(\boldsymbol{\omega}_n;\breve{\mathbf{R}}_\theta)$,

$$\boldsymbol{\omega}_{n,\text{opt}}=\arg\max_{\boldsymbol{\omega}_n^T\boldsymbol{\omega}_n=1}\alpha\mathcal{R}(\boldsymbol{\omega}_n;\breve{\mathbf{R}}_\theta=\boldsymbol{\Sigma}_0^{-1}\mathbf{R}_\theta). \tag{8}$$

Using the scalar Lagrange multiplier, $\lambda_{\text{Lag}}\in R$, we obtain

$$\Gamma_n^2(\boldsymbol{\omega}_n)=\boldsymbol{\omega}_n^T\breve{\mathbf{R}}_\theta\boldsymbol{\omega}_n+\lambda_{\text{Lag}}(\boldsymbol{\omega}_n^T\boldsymbol{\omega}_n-1), \tag{9}$$

where solving the equation $\partial\Gamma_n^2(\boldsymbol{\omega}_n)/\partial\boldsymbol{\omega}_n=0$, we can attain $\boldsymbol{\omega}_{n,\text{opt}}=eig_{\max}(\breve{\mathbf{R}}_\theta)$ as the maximum eigenvector of $\breve{\mathbf{R}}_\theta$ which is corresponding to λ_1, the largest eigenvalue of $\breve{\mathbf{R}}_\theta$.

In the following, we present a more general approach relying on the subspace spanned by the L largest eigenvectors of $\breve{\mathbf{R}}_\theta$.

Let $\boldsymbol{\Omega}_n=[\hat{\boldsymbol{\omega}}_1,\hat{\boldsymbol{\omega}}_2,\cdots,\hat{\boldsymbol{\omega}}_K]$ be an orthogonal matrix whose columns satisfy $\hat{\boldsymbol{\omega}}_k^T\hat{\boldsymbol{\omega}}_{k'}=\delta_{kk'}$ and $\boldsymbol{\Omega}_n^T\boldsymbol{\Omega}_n=\mathbf{I}_K$, where $\delta_{kk'}$ is the Kronecker delta, and $\mathbf{I}_K$ is the identity matrix of order K. We now define a diagonal matrix $\mathbf{G}$=diag($\boldsymbol{g}$), where $\boldsymbol{g}=[g_1,g_2,\cdots,g_K]^T$ satisfies $g_1\ge g_2\ge\cdots\ge g_K\ge 0$. The optimization problem in (8) can be again presented as

$$J(\boldsymbol{\Omega}_n,\mathbf{G})=\text{Tr}(\mathbf{G}\boldsymbol{\Omega}_n^T\breve{\mathbf{R}}_\theta\boldsymbol{\Omega}_n)=\text{Tr}(\boldsymbol{\Omega}_n\mathbf{G}\boldsymbol{\Omega}_n^T\breve{\mathbf{R}}_\theta), \tag{10}$$

where Tr(•) is the trace of a matrix.

When $\boldsymbol{\Omega}_n$ consists of K eigenvectors of $\breve{\mathbf{R}}_\theta$, and $\boldsymbol{\Omega}_n=[\hat{\boldsymbol{\omega}}_{1'},\hat{\boldsymbol{\omega}}_{2'},\cdots,\hat{\boldsymbol{\omega}}_{K'}]$, we have

$$\boldsymbol{\Omega}_n^T\breve{\mathbf{R}}_\theta\boldsymbol{\Omega}_n=\text{diag}(\lambda_{1'},\lambda_{2'},\cdots,\lambda_{K'}), \tag{11}$$

where $\{1',2',\cdots,K'\}$ is a permutation of $\{1,2,\cdots,K\}$ resulting in $\lambda_{1'}>\lambda_{2'}>\cdots>\lambda_{K'}$. The result in (10) now reduces to $J(\boldsymbol{\Omega}_n)=\sum_{k'=1}^{K'}g_{k'}\lambda_{k'}$.

Due to the extremely low duty cycle of the IR-UWB signal, we consider $\boldsymbol{g}'$ with $g_1\ge g_2\ge\cdots\ge g_L\ge g_{L+1}=\cdots=g_K=0$, in which the last $(K-L)$ columns of $\boldsymbol{\Omega}_n$ automatically vanish. Using the newly defined $\mathbf{G}'=\text{diag}(\boldsymbol{g}')$, we have

$$J(\boldsymbol{\Omega}_n,\mathbf{G}')=\text{Tr}(\mathbf{G}'\boldsymbol{\Omega}_n^T\breve{\mathbf{R}}_\theta\boldsymbol{\Omega}_n)=\text{Tr}(\boldsymbol{\Omega}_n\mathbf{G}'\boldsymbol{\Omega}_n^T\breve{\mathbf{R}}_\theta), \tag{12}$$

where L arbitrary mutually orthogonal eigenvectors are used. When $L=1$, $J(\boldsymbol{\Omega}_n,\mathbf{G}')$ reduces to $J(\hat{\boldsymbol{\omega}}_1')=\hat{\boldsymbol{\omega}}_1'^T\breve{\mathbf{R}}_\theta\hat{\boldsymbol{\omega}}_1'$ in (12), under the condition that $g_1=1$ and $\hat{\boldsymbol{\omega}}_1'^T\hat{\boldsymbol{\omega}}_1'=1$. When $g_1=\cdots=g_L=1$, $J(\boldsymbol{\Omega}_n,\mathbf{G}')$ is maximized since $\mathbf{G}'\boldsymbol{\Omega}_n^T$ equivalently consists of the L largest eigenvectors.

IV. Iterative Threshold Tests Based FTE

Subsequent to the CSA, the ITT-based FTE is proposed to refine the TOAE within the j-th subframe with time granularity T_{b}. Since the IR-UWB signal energy might leak from the j-th subframe to the (j–1)-th one, the FTE is performed on the concatenated vector $\breve{\boldsymbol{y}}=[\boldsymbol{y}_{j-1}^T\ \boldsymbol{y}_j^T]^T=[\breve{y}_1,\breve{y}_2,\cdots,\breve{y}_{2M}]^T$.

The proposed ITT has a threefold merit for the TOAE. First, similar to the CSA, the ITT requires no *a priori* channel knowledge. Second, the iterative threshold setting is intrinsically completed in the ITT itself without requiring knowledge of the noise variance. Third, the leading edge sample (LES, the first sample in $\breve{\boldsymbol{y}}$ that contains the first IR-UWB signal component) search algorithm yields a more accurate TOAE than the conventional threshold test (CTT).

Specifically, the ITT is performed in the following steps:

Step 1. The samples $\breve{\boldsymbol{y}}$ are first sorted into $\tilde{\boldsymbol{y}}$ in an ascending order, with $\tilde{\boldsymbol{y}}=[\tilde{y}_1,\tilde{y}_2,\cdots,\tilde{y}_{2M}]^T=[\breve{y}_{1'},\breve{y}_{2'},\cdots,\breve{y}_{(2M)'}]^T$, where $\{1',2',\cdots,(2M)'\}$ is a permutation of $\{1,2,\cdots,2M\}$ resulting in $\tilde{y}_1\le\tilde{y}_2\le\cdots\le\tilde{y}_{2M}$.

Step 2. The first η smallest samples $\{\tilde{y}_i\}_{i=1}^{\eta}$ are assumed to

contain noise energy samples only and form the initial IR-UWB signal-free subset, on which the test iteration begins:

$$\tilde{y}_{i+1} > \frac{1}{i}\sum_{l=1}^{i}\tilde{y}_l\xi, \qquad \eta \le i \le 2M-1, \tag{13}$$

where ξ is the test coefficient based on the previously determined noise-only samples belonging to the observation intervals other than the j-th and $(j-1)$-th subframes.

Step 3. If the first test $(i=\eta)$ of (13) is true, the algorithm stops, and $\breve{\boldsymbol{y}}_{(\mathrm{ITT})}=[\breve{y}_{\eta+1},\breve{y}_{\eta+2},\cdots,\breve{y}_{2M}]^T$ are decided to contain the IR-UWB signal, for which we can find the corresponding $\breve{\boldsymbol{y}}_{(\mathrm{IIT})}=[\breve{y}_{(\eta+1)'},\breve{y}_{(\eta+2)'},\cdots,\breve{y}_{(2M)'}]^T$; otherwise, the test in (13) is performed again with i incremented by 1.

Step 4. The test in (13) is repeated until it is true for some value of $i=\zeta$ or $i=2M-1$ implying all samples are decided to be the noise-only ones after a thorough search over $\tilde{\boldsymbol{y}}$.

Step 5. The final TOAE is obtained as

$$\begin{aligned}\hat{i}_{\mathrm{toa}} &= \arg\max_{i\in\{1,2,\cdots,2M\}} \breve{\boldsymbol{y}}_{(\mathrm{ITT})} - i_{\mathrm{LE}} - 1,\\ \hat{\tau}_{\mathrm{toa}} &= t_s + (j-2)T_{\mathrm{sf}} + (\hat{i}_{\mathrm{toa}} - 0.5)T_b,\end{aligned} \tag{14}$$

where $\breve{\boldsymbol{y}}_{(\mathrm{ITT})}$ and $\tilde{\boldsymbol{y}}_{(\mathrm{ITT})}$ have the same elements but in different orders, and i_{LE} is the number of samples from the determined LES to the maximum sample in $\breve{\boldsymbol{y}}_{(\mathrm{ITT})}$, satisfying

$$\begin{cases}\breve{y}_i \in \breve{\boldsymbol{y}}_{(\mathrm{ITT})}, \text{when } i=\hat{i}_{\mathrm{toa}}, \hat{i}_{\mathrm{toa}}+1,\cdots,\hat{i}_{\mathrm{toa}}-\hat{i}_{\mathrm{LE}}-1,\\ \breve{y}_i \notin \breve{\boldsymbol{y}}_{(\mathrm{ITT})}, \text{when } i=\hat{i}_{\mathrm{toa}}-1.\end{cases} \tag{15}$$

In this way, the problem of TOAE is accomplished in a fine-scale with accuracy defined by the mean absolute error (MAE),

$$\varepsilon_{abs}(i_{\mathrm{toa}}) = E[\left|\hat{i}_{\mathrm{toa}} - i_{\mathrm{toa}}\right|] = \sum_{i=1}^{2M} P_{\mathrm{toa}}^{(i)} \left|\hat{i}_{\mathrm{toa}} - i_{\mathrm{toa}}\right|, \tag{16}$$

where $P_{\mathrm{toa}}^{(i)}$ is the probability of the i-th sample being determined as the first arriving IR-UWB signal-present sample.

V. Simulations

The simulation parameters are fixed as T_{f}=200 ns, W=5 GHz, T_{b}= 1 ns, N=4, M=50, K=10, m=5, η=16, and ξ=1.582. Each channel realization has a TOA uniformly distributed within [0, T_{f}]. Note that $\mathbf{u}_0$ and $\boldsymbol{\Sigma}_0$ need to be estimated to obtain the blind estimation of $\breve{\mathbf{R}}_\theta$, based on previously received P=100 statistics $\{\breve{\mathbf{Y}}^{(p)}=[\boldsymbol{y}_1^{(p)},\cdots,\boldsymbol{y}_{j-2}^{(p)},\boldsymbol{y}_{j+1}^{(p)},\cdots,\boldsymbol{y}_N^{(p)}]\}_{p=i-P+1}^{i}$, where i is the frame index of the current statistics.

Figure 1(a) gives the performance of correctly identifying the IR-UWB signal-present subframe in the IEEE802.15.3a CM1 channel. We find the practically optimal L is 2 for CM1 to CM4. The RQ-based CSA scheme has a much higher detection probability than the non-weighted method. Figure 1(b)

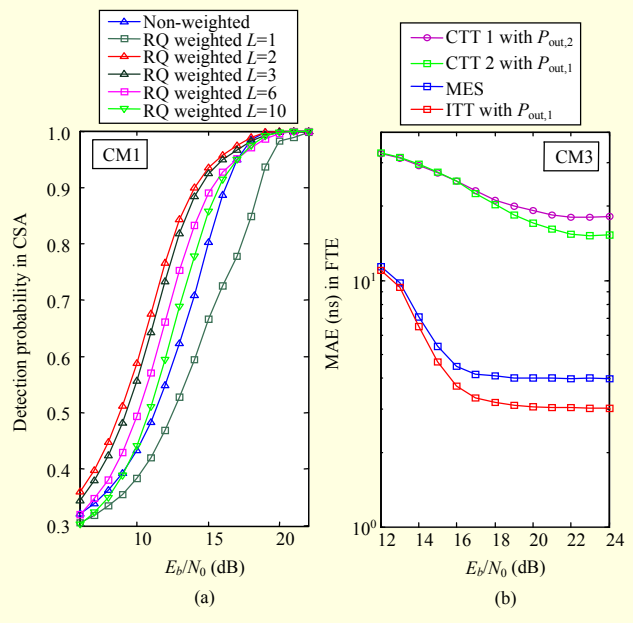

Fig. 1. (a) Detection probabilities in CSA and (b) MAE in FTE.

gives the MAE performance of the ITT in the CM3 channel, demonstrating a more refined TOAE accuracy than the CTT, and maximum energy selection approaches [4], which also benefited significantly in the CSA stage. Outlying probabilities $P_{\mathrm{out},1}$=10% and $P_{\mathrm{out},2}$=15% are used for both the threshold-setting in CTT and coefficient-setting in ITT.

VI. Conclusion

An energy-detection-based blind IR-UWB TOAE scheme was proposed. The coarse and fine TOAE strategies were seamlessly integrated into one complete and compact entity to attain the TOAE with improved signal detection probability and TOAE accuracy compared to conventional methods.

References

[1] A. Rabbachin and I. Oppermann, "Synchronization Analysis for UWB Systems with a Low-Complexity Energy Collection Receiver," *Proc. IEEE UWB Syst. Tech. Conf.*, 2004, pp. 288-292.

[2] I. Guvenc, Z. Sahinoglu, and P.V. Orlik, "TOA Estimation for IR-UWB Systems with Different Transceiver Types," *IEEE Trans. Microw. Theory Tech.*, vol. 54, no. 4, 2006, pp. 1876-1886.

[3] R.E. Prieto, "A General Solution to the Maximization of the Multidimensional Generalized Rayleigh Quotient Used in Linear Discriminant Analysis for Signal Classification," *Proc. IEEE ICASSP*, 2003, pp.157-160.

[4] I. Guvenc and Z. Sahinoglu, "Threshold-Based TOA Estimation for Impulse Radio UWB Systems," *Proc. IEEE ICUWB*, 2005, pp. 420-425.